J. Environ. Nanotechnol.
Volume 8, No.1(2019) pp. 25 - 33
ISSN (Print): 2279-0748
ISSN (Online): 2319-5541
doi:10.13074/jent.2019.03.191345

Carbon Dioxide Decomposition Over $AlPO_4$ Based Molecular Sieves

S. Siva Sankari[1], M. A. Mary Thangam[2], Chellapandian Kannan[3]*

[1,2,*3]*Department of Chemistry, Manonmaniam Sundaranar University, Abishekapatti, TN, India.*

Received: 08.11.2018 *Accepted: 25.12.2018*

Abstract

Carbon dioxide is the most prevalent greenhouse gas that traps heat and raises the global temperature. To minimize this undesirable climate change, the solid acid catalysts are to be used for the decomposition of CO_2. Aluminophosphate molecular sieves have void applications in the field of catalysis and adsorption. Metal incorporated aluminophosphate molecular sieves like Magnesium aluminophosphate and Manganese aluminophosphate are synthesizeod using low cost n-butyl amine as new template which is of high activity in the decomposition of CO_2 into CO and O_2. The FT-IR spectrum confirms the formation of tetrahedral framework of the materials. Powder X-ray diffraction pattern of calcinated Mg-$AlPO_4$ and Mn-$AlPO_4$ proved the well crystalline nature of the material. The morphology of the material is explained by using SEM analysis. The BET surface area of calcinated Mg-$AlPO_4$ and Mn-$AlPO_4$ confirmed the mesoporous nature of the materials. The decomposition of carbon dioxide has been carried out in a catalytic reactor over Mg-$AlPO_4$ and Mn-$AlPO_4$.The catalytic reaction conditions like temperature, flow rate, catalyst dosage and time on stream are determined for the maximum conversion of CO_2. The conversion and product selectivity depends on the acidity and pore size of the catalysts.

Keywords: *Carbon dioxide decomposition; n-butyl amine; Mg-$AlPO_4$; Mn-$AlPO_4$.*

1. INTRODUCTION

Global warming is caused by increased emissions of greenhouse gases (mainly Carbon dioxide) into the atmosphere. Generally, polymeric adsorbents, zeolites, silica gels, activated carbons, and molecular sieves have been extensively used as selective adsorbents because of their controllable pore structures and surface properties, which can be used to selectively capture CO_2 (Anastas *et al.* 2001; Taguchi and Schuth, 2005). Among these adsorbents, molecular sieves have the ability to selectively absorb specific components of gaseous mixtures because of their porous structures, which consist of relatively uniform pores. The porous solid acid materials are green catalysts for organic reactions. Solid acids are generally categorized by 'Brownsted acids' or 'Lewis acids' (Liu *et al.* 2006). They are based on micelle-template silica's and other mesoporous high surface area support materials are beginning to play a significant role in the greening of fine and speciality chemicals manufacturing processes (Ruthven, 1984). A solid acid catalyst has an advantage such as an easy operation for isolating a product after the reaction (Smit and Maesen, 2008). Heteroatom-containing aluminophosphate molecular sieves as a prime class of heterogeneous single-site solid catalysts. Aluminophosphate play an important role in the field of catalysis and adsorption (Pai *et al.* 2008). The application depends on its pore size, acidity, surface area and stability. In order to increase the catalytic activity of mesoporous $AlPO_4$ molecular sieves, the metal ions are incorporated into the framework of $AlPO_4$ (Gao *et al.* 1997). In this work, we prepare the metal incorporated aluminophosphate molecular sieves like Magnesium aluminophosphate and Manganese aluminophosphate by sol-gel method using n-butyl amine as a new template. The catalytic activity of the catalysts has been studied by carbon dioxide decomposition reaction. The experimental conditions like temperature, flow rate, catalyst dosage and time on stream are optimized for maximum conversion of CO_2. The regeneration of catalysts is performed by thermal method in the presence of air.

**** Chellapandian Kannan***
email: *chellapandiankannan@gmail.com*

2. EXPERIMENTAL METHODS

2.1 Materials

The chemicals for the synthesis of mesoporous aluminophosphate are aluminium hydroxide (Merck, GR), Orthophosphoric acid (Nice, GR) and n-butyl amine (Loba chemie, GR). The metal sulphates used for the isomorphous substitution in the $AlPO_4$ framework are Magnesium sulphate and Manganese sulphate (Merck, GR) respectively.

2.2 Characterisation

The Fourier Transform Infrared (FT-IR) measurements of samples are recorded by JASCO-410 FT-IR model spectrophotometer by using KBr pellet technique. X-ray diffraction patterns are recorded on a PANalytical X'Pert Pro Powder X'Celerator Diffractometer using Cu-Kα radiation (λ= 1.5406 ´) with a voltage 40 kV and current 30mA. The SEM images are recorded by Carl Zeiss Evo 18 Scanning electron microscope with the voltage 20 kV. The surface area of the samples was obtained by the Brunauer-Emmett Teller (BET) method and the pore size distribution was calculated from the BJH method. Nitrogen adsorption-desorption measurements are made using Smart instruments CO. PVT.LTD, Smart Sorb 92/93, the sample is out gassed at 200°C for one hour.

2.3 Synthesis of Metal ion substituted Aluminophosphate molecular sieves

Aluminium hydroxide and Orthophosphoric acid are chosen as the source material for aluminium and phosphorous respectively. 9.8 ml of n-butylamine is dissolved in 150ml of deionised water. Then 7.8g of aluminium hydroxide is added in 100ml of water and add slowly into the template solution and stirred it for one hour. About 9.8 g (5.2 ml) of orthophosphoric acid is dissolved in 50 ml of water and isomorphous substitution of metal ions taking place by adding 0.02 mole of magnesium sulphate (2.406 g) or manganese sulphate (3.02 g) into the above mixture and stirred continuously for 2 hours to attain homogeneous mixture. The resulting mixture is dried in hot air oven at 120°C and washed thoroughly with deionised water until the pH of the discarded solution become neutral. The solid is then filtered and dried at 120 °C in a hot air oven. The gel compositions are 0.98 Al_2O_3: P_2O_5: n-A:0.02 MgO:300 H_2O and 0.98 Al_2O_3: P_2O_5: n-BA: 0.02 MnO: 300 H_2O. The synthesized material is calcinated at 400 °C for 4 hours to remove the organic template present in the pores of the molecular sieves.

2.4 Catalytic reactor

The catalytic activity studies are carried out in gas phase. The required amount of calcinated catalysts are taken in a U-shaped tube. One end of the tube is connected to carbon dioxide cylinder and the other end is connected to the bottle containing silica gel to absorb moisture (Fig. 1).

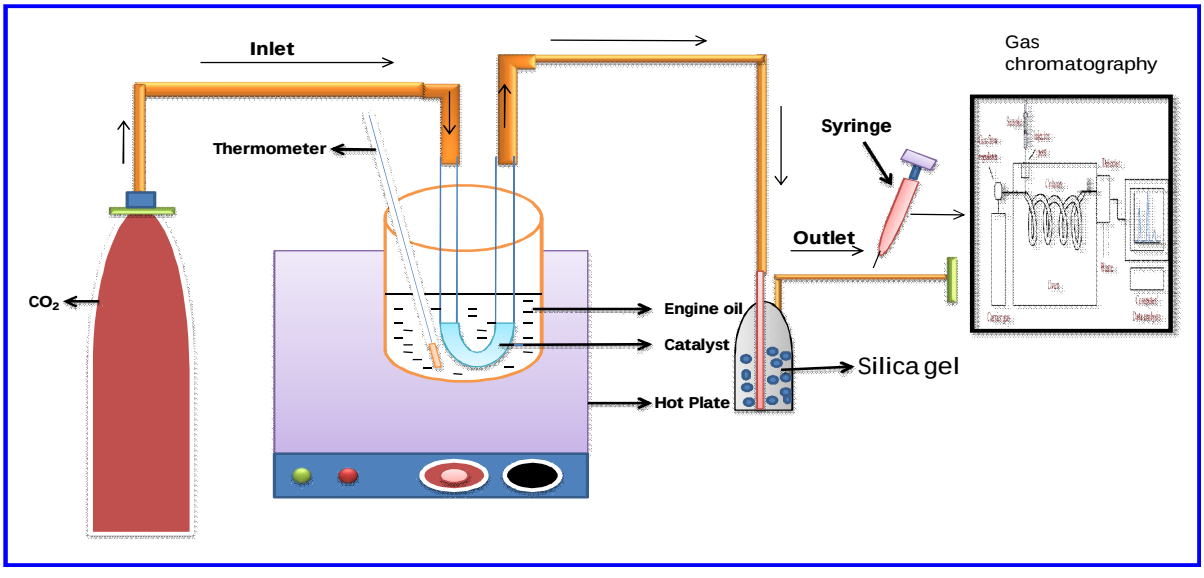

Fig. 1: Catalytic reactor for the decomposition of CO_2

The carbon dioxide flowed into the catalyst and the decomposition of CO_2 takes place to produce different products. The reaction products are taken from the outlet tube using syringe and the products are analyzed by gas chromatography.

3. RESULT & DISCUSSION

3.1 FT-IR spectrum

The Fig. 2(a) and 3(a) shows the strong broad band at 3400-3600 cm^{-1} which is assigned to the O-H vibration of water molecule that present in the as-synthesized sample whereas in calcinated sample Figure 2(b) and 3(b) the –OH bond becomes weak. The asymmetric stretching vibrations of tetrahedral aluminophosphate are observed near 1100 cm^{-1} (Campelo *et al.* 2003). The symmetric stretching and bending mode is observed near 700 cm^{-1} and 500 cm^{-1} (Campelo *et al.* 1986).

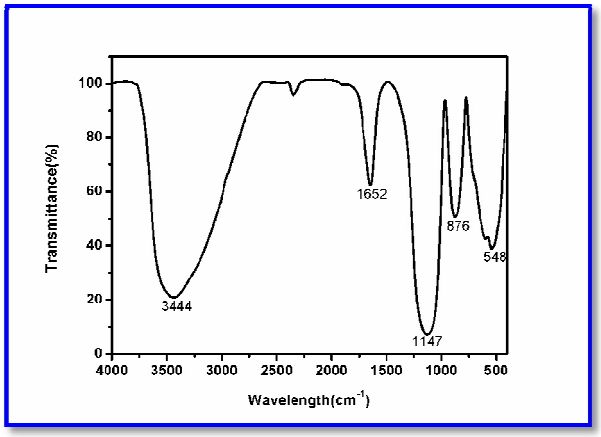

Fig. 2(a): FT-IR spectrum of asynthesized Mg-$AlPO_4$

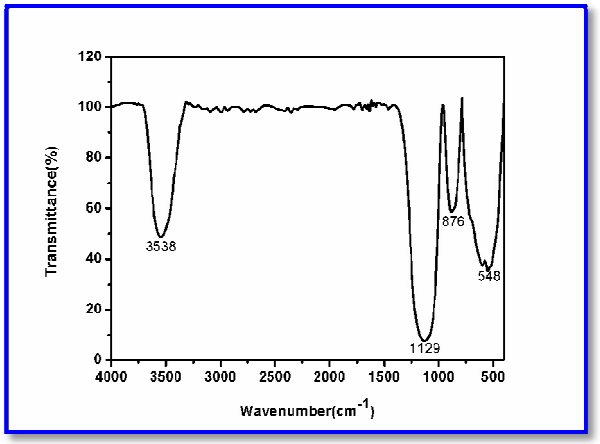

Fig. 2(b): FT-IR spectrum of calcinated Mg- $AlPO_4$

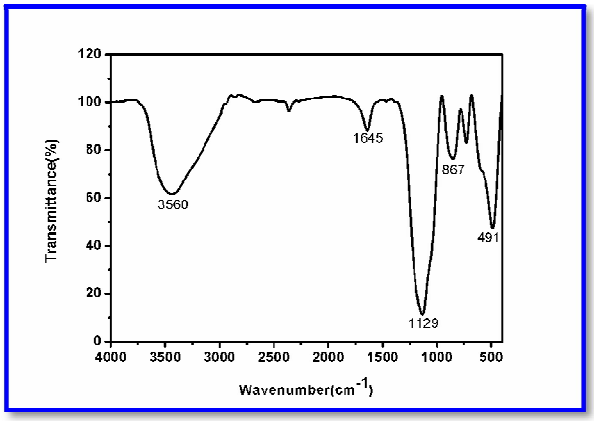

Fig. 3(a): FT-IR spectrum of asynthesized Mn-$AlPO_4$

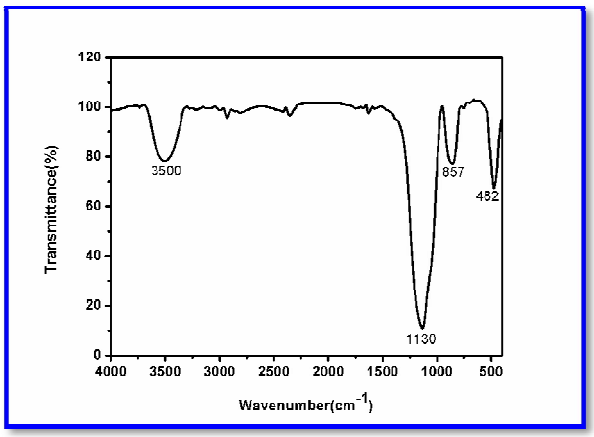

Fig. 3(b): FT-IR spectrum of calcinated Mn-$AlPO_4$

The C-H deformation band, C-N band and N-H bending band at 1460cm^{-1}, 1350 cm^{-1} and 1500 cm^{-1} are present in as-synthesized sample whereas in calcinated sample these bands are absent. This proved that there is complete removal of template molecule from the as-synthesized sample after calcinations. The peaks between 1000 cm^{-1} and 1200 cm^{-1} region confirms the presence of metal ions into the tetrahedral framework (Cheralathan *et al.* 2000).

3.2 Powder X-Ray diffraction analysis

The powder X-ray diffraction pattern of calcinated Mg-$AlPO_4$ and Mn-$AlPO_4$ are shown in Figure 4 and 5 which proved the well crystalline nature of the material (Tanev and Pinnavaia, 1995). The d–spacing values of the materials are closely matched with the JCPDS files (881680 & 511755) also it confirms that the materials are in hexagonal structure (Table 1). The average crystal size of Mg-$AlPO_4$ and Mn-$AlPO_4$ are 7.60nm and 18.91nm respectively.

Table 1. XRD parameters for Mg-$AlPO_4$ and Mn-$AlPO_4$

Catalyst	Lattice	System	h k l	2ɵ	d-spacing(Å)	
					Standard	Observed
Mg-$AlPO_4$	Primitive	Hexagonal	6 2 2	45.9433	1.9722	1.97537
			0 0 6	67.0747	1.3944	1.39541
Mn-$AlPO_4$	Primitive	Hexagonal	2 1 0	20.3601	4.3294	4.36193
			2 1 1	21.5084	4.1139	4.13158
			0 0 7	45.5887	1.9057	1.98990
			3 2 8	66.7122	1.4071	1.40211

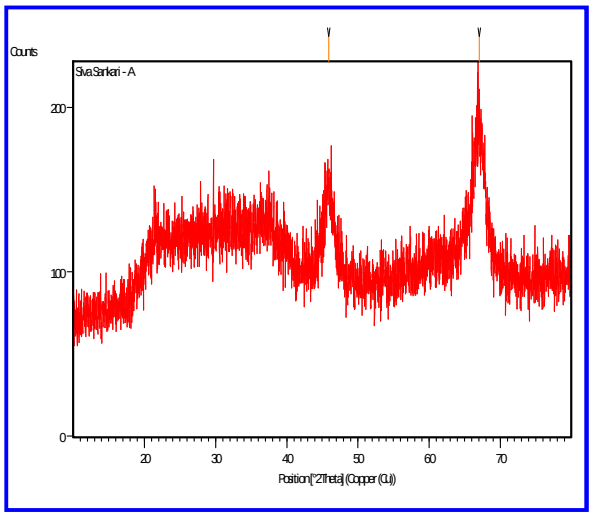

Fig. 4: XRD pattern of calcinated Mg-$AlPO_4$

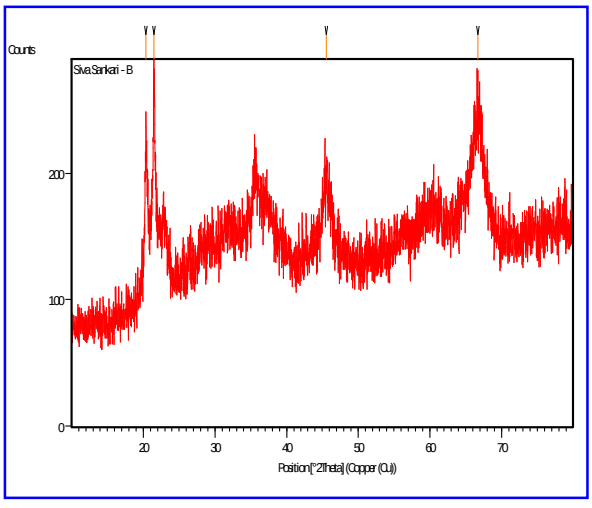

Fig. 5: XRD pattern of calcinated Mn-$AlPO_4$

3.3 Scanning electron microscopic analysis

SEM images of calcinated Mg-$AlPO_4$ and Mn-$AlPO_4$ are shown in Figure 6 and 7 respectively. The SEM images clearly represented the crystalline nature of the metal ion incorporated $AlPO_4$ materials. All the materials have various particle sizes in nanoscale. The variation in morphology and pore creation among the Mg-$AlPO_4$ and Mn-$AlPO_4$ is an evidence for the metal ions incorporation in the tetrahedral framework of the molecular sieves (Hardie *et al.* 2005).

3.4 Surface area and pore size distribution

The BET surface area of calcinated Mg-$AlPO_4$ and Mn-$AlPO_4$ are 71.66 m^2/g and 49.39 m^2/g and their pore diameters are 10 nm and 12 nm respectively. This confirms the mesoporous nature of the materials.

4. CATALYTIC APPLICATION

4.1 Decomposition of carbon dioxide over mesoporous $AlPO_4$ based molecular sieves

The decomposition of carbon dioxide has been carried out over metal ion incorporated catalysts like Mg-$AlPO_4$ and Mn-$AlPO_4$ under controlled experimental conditions, the carbon dioxide is decomposed into carbon monoxide and oxygen. The optimum experimental conditions like temperature, flow rate, catalyst dosage and time on stream are determined for find out the maximum conversion of CO_2 and product selectivity.

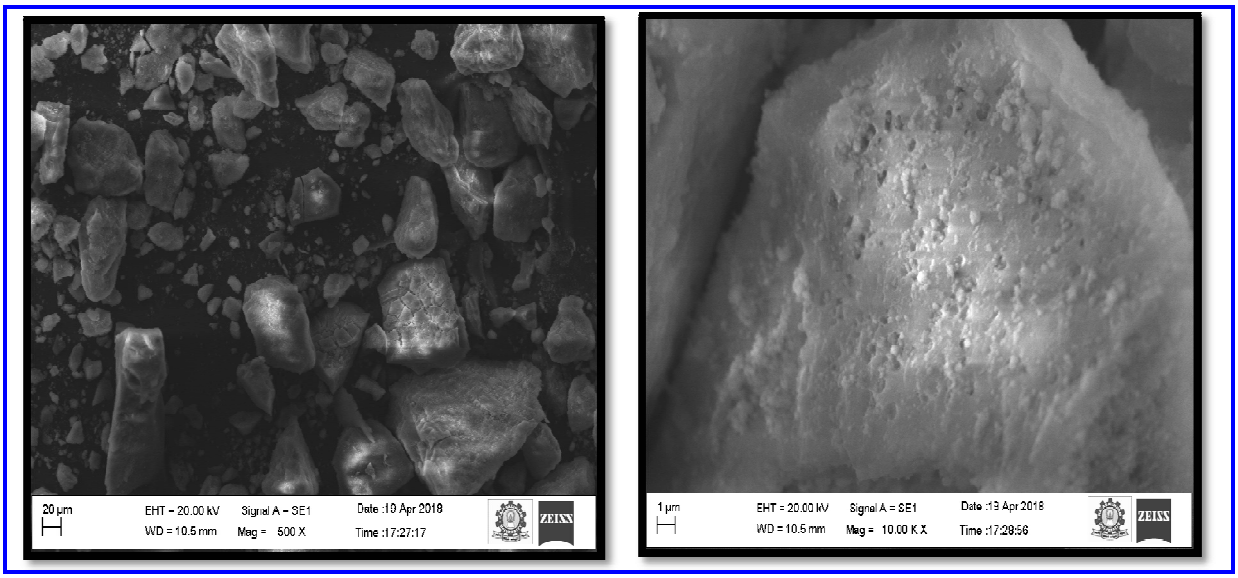

Fig. 6: SEM images of Mg-$AlPO_4$

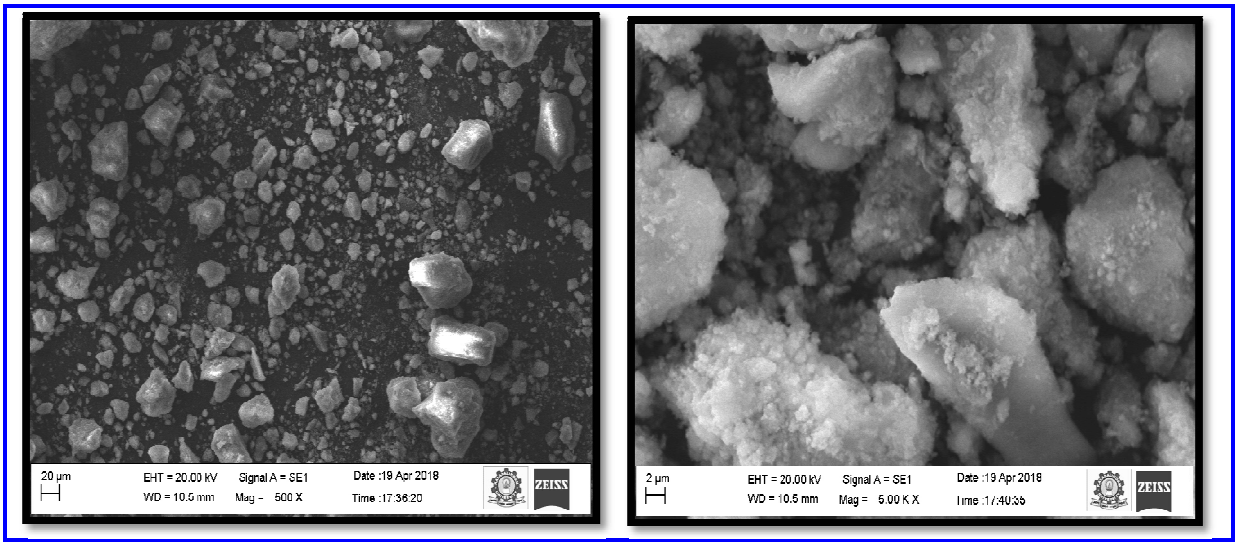

Fig. 7: SEM images of Mn-AlPO

4.1.1 Effect of temperature

The influence of temperature on the decomposition of CO_2 has been studied on 0.5g of catalysts like Mg-$AlPO_4$ and Mn-$AlPO_4$ at the temperature range of 60°, 70°, 80°, 150° and 200°C are shown in Figure 8. The percentage of conversion of carbon dioxide and the product selectivity with respect to temperature are shown in Table 2. In Mg-$AlPO_4$, the maximum conversion is observed at 60°C, further increase of temperature there is no significant conversion has been found. This proved the high catalytic activity of the catalyst. In Mn-$AlPO_4$, the maximum conversion of carbon dioxide is found at 60°C and further increased of temperature conversion decreases. This proved that the catalytic activity of Mn-$AlPO_4$ decreases with increased of temperature. The selectivity of oxygen decreases with decreasing of conversion, but carbon monoxide selectivity increases with decrease of conversion. This may be due to the adsorption of oxygen inside the pores of the catalysts. This behaviour depends on the nature of the catalyst.

Table 2. Effect of temperature over $MAlPO_4$

Catalyst	Temperature (°C)	Conversion (%)	Product selectivity (%)	
			CO	O_2
Mg-$AlPO_4$	60	99.7986	44.5147	55.4855
	70	99.6991	48.9603	51.9027
	80	99.5456	50.7007	49.2994
	150	99.5356	51.1699	48.8301
	200	99.3237	48.0975	51.9027
Mn-$AlPO_4$	60	74.0109	52.3016	47.6983
	70	36.5067	76.2409	23.6466
	80	32.3018	94.7786	5.2214
	150	25.9584	93.0443	6.9557
	200	26.4061	91.8759	8.1243

Time: 1h, Catalyst amount: 0.5g, Flow rate: 0.5ml/min

Table 3. Effect of flow rate over $MAlPO_4$

Catalyst	Flow rate (ml/min)	Conversion (%)	Product selectivity (%)	
			CO	O_2
Mg-$AlPO_4$	0.5	99.3237	44.5147	55.4855
	1.5	15.0212	88.7905	11.2088
	2.5	12.8044	92.6415	7.3574
Mn-$AlPO_4$	0.5	74.0109	52.3016	47.6983
	1.5	11.0298	81.7825	18.2179
	2.5	13.3026	88.0046	11.9962

Time: 1h, Catalyst amount: 0.5g, Temperature: 60 °C

4.1.2 Effect of flow rate

The effect of flow rate on the decomposition of carbon dioxide over 0.5 g of Mg-$AlPO_4$ and Mn-$AlPO_4$ catalysts has been studied from 0.5 to 2.5 ml per minute are shown in Fig 9. The percentage of conversion and product selectivity with respect to flow rate are shown in Table 3. The maximum conversion of carbon dioxide is observed at 0.5 ml per minute. Further increases of flow rate, the percentage of conversion decreases. The percentage of conversion increases with a decreased of CO_2 flow rate due to the longer residence time in the catalytic bed. The selectivity of oxygen decreases with decreasing of conversion, but carbon monoxide selectivity increases with decrease of conversion. This may be due to the adsorption of oxygen inside the pores of the catalysts. This behaviour depends on the nature of the catalyst.

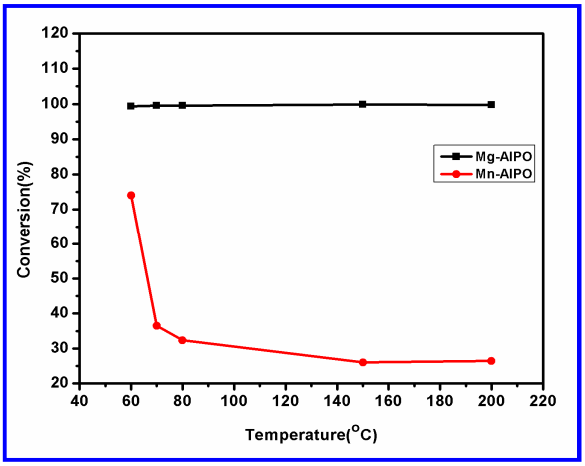

Fig. 8: Effect of temperature on decomposition of CO_2 over $MAlPO_4$

4.1.3 Effect of catalyst dosage

The effect of catalyst dosage on carbon dioxide decomposition reaction over Mg-$AlPO_4$ and Mn-$AlPO_4$ catalysts has been studied from 0.5 g to 1.5 g are shown in Fig. 10. The percentage of conversion of carbon dioxide and selectivity of the products with respect to catalyst dosage are shown in Table 4. The maximum conversion is observed at 0.5 g, further increasing of catalyst dosage, the percentage of conversion decreases. At lower catalyst dosage, the conversion of CO_2 will easily occur; while at higher catalyst dosage, the recombination of carbon monoxide and oxygen takes place to form carbon dioxide in the catalytic bed due to the long pathway of the carbon monoxide and oxygen in the reactor. The selectivity of oxygen decreases with decreasing of conversion, but carbon monoxide selectivity increases with decrease of conversion. This may be due to the adsorption of oxygen inside the pores of the catalysts. This behaviour depends on the nature of the catalyst.

4.1.4 Effect of time on stream

From all the above experimental data, it is found to clear that the maximum conversion of carbon dioxide is observed under the following respective experimental conditions.

Reaction temperature: 60°C Catalyst dosage: 0.5 g
Flow rate: 0.5 ml

The effect of time on stream has been carried out over Mg-$AlPO_4$ and Mn-$AlPO_4$ up to 5 hours (Table 5). The carbon dioxide decomposition decreases with increased of time (Fig. 11). This may be due to the pressure of carbon dioxide in the reactor bed. The carbon dioxide flow is arrested at the outlet. Hence pressure is developed in the catalytic bed. So the carbon dioxide reaction reduces with increased of flow rate. The selectivity of oxygen decreases with decreasing of conversion, but carbon monoxide selectivity increases with decrease of conversion. This may be due to the adsorption of oxygen inside the pores of the catalysts. This behaviour depends on the nature of the catalyst.

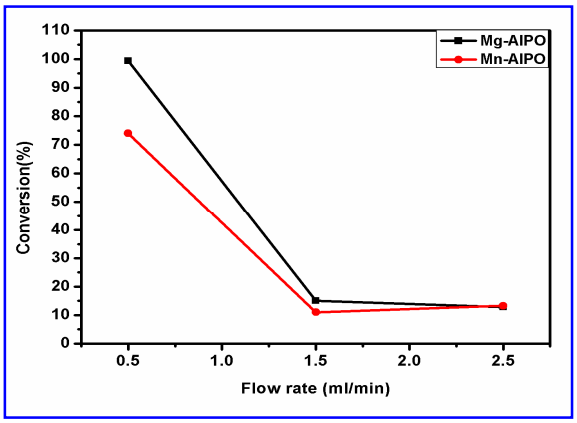

Fig. 9: Effect of flow rate on decomposition of CO_2 over $MAlPO_4$

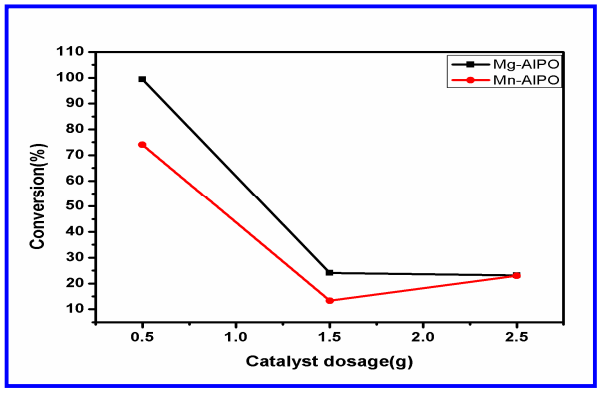

Fig. 10: Effect of catalyst dosage on decomposition of CO_2 over $MAlPO_4$

Table 4. Effect of Catalyst dosage over $MAlPO_4$

Catalyst	Catalyst dosage(g)	Conversion (%)	Product selectivity (%)	
			CO	O_2
Mg-$AlPO_4$	0.5	99.3237	44.5147	55.4855
	1.5	24.1327	76.4858	23.5141
	2.5	23.1289	72.9442	27.0558
Mn-$AlPO_4$	0.5	74.0109	52.3016	47.6983
	1.5	13.3290	78.3547	21.6452
	2.5	22.9897	75.3485	24.6515

Time: 1h, Temperature: 60°C, Flow rate: 0.5ml/minute

Table 4. Effect of time on stream over $MAlPO_4$

Catalyst	Time (h)	Conversion (%)	Product selectivity (%)	
			CO	O_2
Mg-$AlPO_4$	1	24.6846	91.2034	8.7966
	2	26.5441	74.7119	25.2881
	3	22.2317	38.0924	22.2317
	4	16.0788	58.5435	41.4565
	5	25.0261	61.8846	38.1953
Mn-$AlPO_4$	1	18.2146	83.7317	16.2682
	2	12.8382	77.9689	22.0311
	3	16.8197	92.7841	7.2159
	4	18.6417	85.9734	14.0373
	5	26.4486	88.2549	11.7450

Time: 1h, Temperature: 60°C, Flow rate: 0.5ml/minute

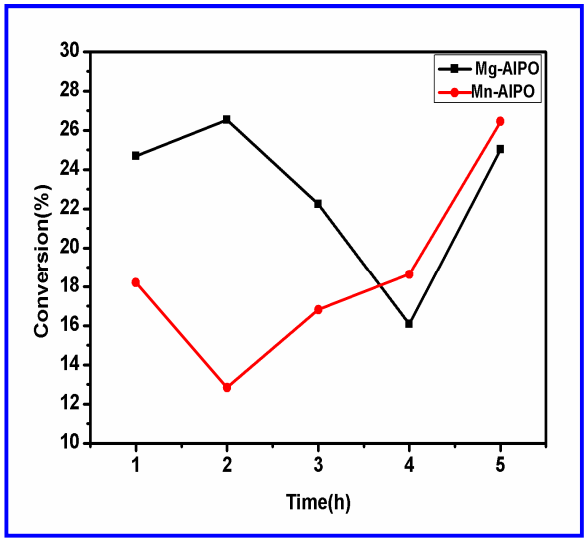

Fig. 11: Effect of time on stream on decomposition of CO_2 over $MAlPO_4$

5. CONCLUSION

The mesoporous Mg-$AlPO_4$ and Mn-$AlPO_4$ are synthesized by sol gel method using n-butyl amine as a new template. The synthesized materials are characterized by Powder X-Ray Diffraction, Fourier Transform Infrared technique and Scanning electron microscope technique. These techniques proved the formation of $AlPO_4$ materials. The catalytic activity of the catalysts has been studied by carbon dioxide decomposition reaction. The decomposition of carbon dioxide has been carried out in a catalytic reactor over Mg-$AlPO_4$ and Mn-$AlPO_4$. The experimental conditions like temperature, flow rate, catalyst dosage and time on stream are optimized for maximum conversion of CO_2. Carbon dioxide molecule is converted into carbon monoxide and oxygen. The decomposed products are analyzed by Gas Chromatography. The decomposition of carbon dioxide by the synthesized material is very effective even at very low temperature (60 °C). Above 90% decomposition of carbon dioxide is observed over Mg-$AlPO_4$ whereas 70% decomposition of carbon dioxide is observed over Mn-$AlPO_4$ material. This observation proved that Mg-$AlPO_4$ is the best catalyst than Mn-$AlPO_4$.

REFERENCES

Anastas, P. T., Kirchhoff, M. M. and Willia, T. C., Catalysis as a foundational pillar of green chemistry, *Applied Catalysis A General*, 221(1-2), 03-13(2001). doi:10.1016/S0926-860X(01)00793-1

Campelo, J. M., Jaraba, M., Luna, D., Luque, R., Marinas, J. M. and Romero, A. A., Effect of phosphate precursor and organic additives on the structural and catalytic properties of Amorphous Mesoporous AlPO4 Materials, *Chem. Mater*., 15, 3352-3364**(2003)**. doi:10.1021/cm030206+

Campelo, M., Marinas, J. M., Mendioroz, S. and Pajares, J. A., Texture and surface chemistry of aluminium phosphates, *J. Catal.*, 101(2), 484-495**(1986)**. doi:10.1016/0021-9517(86)90275-7

Cheralathan, K. K., Kannan, C., Arabindoo, B., Palanichamy, M. and Murugesan, V., Ethylation of toluene over aluminiophosphate molecular sieves in the vapour phase, *Ind. J. Chem. Tech.*, 39(9), 921-927**(2000)**.

Gao, Q., Chen, J., Xu, R. and Yue, Y., Synthesis and characterization of a family of amine-intercatalated lamellar aluminophosphates from alcoholic system, *Chem. Mater*. 9(2), 457-462**(1997)**. doi:10.1021/cm9602611

Hardie, S. M. L., Garnett, M., Fallick, A. E., Rowland, A. P., Carbon-dioxide capture using a zeolite molecular sieve sampling system for isotopic (13C and 14C) studies of respiration, *Radiocarbon*, 47, 441-451(**2005)**. doi: 10.1017/S0033822200035220

Liu, Y., Lotero, E. and Godwin, J. G., Jr., Effect of water on sulfuric acid catalyzed esterification, *J. Mol. Catal. A-Chem*., 245(1-2), 132-140**(2006)**. doi:10.1016/j.molcata.2005.09.049

Pai, S. M., Newalkar, B. L. and Choudary, N. V., Microwave-hydrothermal synthesis and characterization of silico-aluminophosphate molecular sieve:SSZ-51, *Micropor. Mesopo. Mat*., 112, 357-367**(2008)**. doi:10.1016/j.micromeso.2007.10.010

Ruthven, D. M., *Principle of adsorption & adsorption processes*. John Wilev & sons. **1984**.

Smit. B. and Maesen. T. L. M.. Towards a molecular understanding of shape selectivity, *Nature*, 451, 671-678(2008). doi:10.1038/nature06552

Taguchi, A. and Schuth, F., Ordered mesoporous materials in catalysis, *Microporous Mesoporous Mater., 77(1),* 01-45(2005). doi:10.1016/j.micromeso.2004.06.030

Tanev, P. T., Pinnavaia, T. J., A neutral templating route to mesoporous molecular sieves, *Science*, 267(5199), 865-867(**1995)**.